SCIENCE CHINA Materials

REVIEW

mater.scichina.com link.springer.com

Published online 5 September 2017 | doi: 10.1007/s40843-017-9105-3
Sci China Mater 2017, 60(9): 793–810

Design and tailoring of patterned ZnO nanostructures for energy conversion applications

Haonan Si[1†], Zhuo Kang[1†], Qingliang Liao[1], Zheng Zhang[1], Xiaomei Zhang[2], Li Wang[3*] and Yue Zhang[1,4*]

ABSTRACT **ZnO is a typical direct wide-bandgap semiconductor material, which has various morphologies and unique physical and chemical properties, and is widely used in the fields of energy, information technology, biomedicine, and others. The precise design and controllable fabrication of nanostructures have gradually become important avenues to further enhancing the performance of ZnO-based functional nanodevices. This paper introduces the continuous development of patterning technologies, provides a comprehensive review of the optical lithography and laser interference lithography techniques for the controllable fabrication of ZnO nanostructures, and elaborates on the potential applications of such patterned ZnO nanostructures in solar energy, water splitting, light emission devices, and nanogenerators. Patterned ZnO nanostructures with highly controllable morphology and structure possess discrete three-dimensional space structure, enlarged surface area, and improved light capture ability, which realize the efficient carrier regulation, achieve highly efficient energy conversion, and meet the diverse requirements of functional nanodevices. The patterning techniques proposed for the precise design of ZnO nanostructures not only have important guiding significance for the controllable fabrication of complex nanostructures of other materials, but also open up a new route for the further development of functional nanostructures.**

Keywords: patterned ZnO nanorod arrays, laser interference lithography, optical lithography, energy conversion devices

INTRODUCTION

Semiconductor materials have attracted considerable research interest because of their broad applications in information transmission, detectors, monitors, lasers, and many other fields [1–3]. The first and second generations of semiconductor materials, based on silicon and gallium arsenide, respectively, have contributed to the rapid development of the computer electronics and mobile communication industries [4–6]. However, owing to the limitation of material properties, the devices based on these semiconductor materials cannot operate at high temperatures [7]. Their anti-radiation performance and emission wavelength range are also unable to meet the increasing needs of societal development [8]. As a representative of the third generation of semiconductor materials, gallium nitride (GaN) has been widely used in short wavelength optoelectronic devices and high-power/high-frequency electronic devices, owing to its wide bandgap, high breakdown voltage, and strong radiation resistance [9,10]. Zinc oxide (ZnO) is another wide-bandgap semiconductor, which has a similar crystal structure to GaN and has attracted considerable interest over the past years [11,12].

As a typical direct bandgap semiconductor, ZnO is a potential candidate material for photoelectronic applications, owing to its excellent physical and chemical properties, such as high electron mobility, excellent environmental stability, and high thermal conductivity [13,14]. ZnO exhibits the piezoelectric effect and excellent photocatalytic performance [15,16]. The large exciton binding energy of ZnO facilitates efficient exciton emission at room temperature or higher temperatures. Generally, the properties of ZnO can be further optimized by

[1] State Key Laboratory for Advanced Metals and Materials, School of Materials Science and Engineering, University of Science and Technology Beijing, Beijing 100083, China
[2] Department of Mechanical Engineering, Tokyo Institute of Technology, Tokyo, Japan
[3] Civil and Environment Engineering School, University of Science and Technology Beijing, Beijing 100083, China
[4] Beijing Municipal Key Laboratory of New Energy Materials and Technologies, University of Science and Technology Beijing, Beijing 100083, China
[†] These authors contributed equally to this work.
[*] Corresponding authors (emails: wangli@ces.ustb.edu.cn (Wang L); yuezhang@ustb.edu.cn (Zhang Y))

doping with various elements [17,18]. The incorporation of Al, Ga, and In reduces the lattice energy of ZnO [19,20]. In particular, the addition of Ga and In can improve the conductivity of ZnO and enhance the stability of its crystal structure [21]. The addition of Al, Ga, and In can further increase the bandgap and conductivity of ZnO without sacrificing its transmittance. The mechanical and electrical properties can be enhanced by Sb doping. The incorporation of transition-metal elements (Sc, Mn, Ti, Co, Ni, Cu, etc.) into ZnO will form diluted magnetic semiconductors or semimagnetic semiconductors [22–24]. The electrical properties of ZnO can be controlled by precisely tuning the dopant concentration [25]. Additionally, the elements of N, P, and others have been used as effective dopants to obtain p-type semiconductors [26]. However, it is generally difficult to achieve bipolar doping for wide-bandgap semiconductors. Furthermore, a variety of ZnO nanostructures have been synthesized by low-cost and low-temperature methods [27]. Among the obtained nanostructures, ZnO nanorods (NAs) can provide an electron transport pathway for the efficient separation of photogenerated electron–hole pairs [28–30]. ZnO NAs have a large surface area, which is conducive to compositing with other materials [17]. The light absorption performance is higher than other structures, because of the light scattering effect. Therefore, ZnO NAs have been widely used in optoelectronic, electrochemical, and electronic devices, such as nanogenerators [31–34], sensors [35–38], light-emitting diodes [39,40], ultraviolet (UV) detectors [41–45], solar cells [46–49], field emission devices [50,51], and biosensors [52–55].

ZnO materials are easy to synthesize and have plentiful preparation methods, which can be divided into the vapor-phase, solution-phase, and solid-phase growth methods, according to the state of the synthetic phase [56–59]. Regarding the ZnO NAs, a wide range of fabrication techniques, such as metal-organic chemical vapor deposition, chemical vapor deposition, pulsed laser deposition, electrochemical deposition, and hydrothermal methods, have been developed [60–62]. However, the ZnO NAs synthesized by traditional vapor-phase and solution-phase growth methods have several drawbacks, such as poor orientation, different space and length of nanorods, and less morphology homogeneity. These ZnO NAs resulted in poor electrode contact, leakage current, large reverse current, and poor stability, which limit the further improvement of the performance and lifetime of the devices [63]. In order to solve the above problems, patterning technology was widely used in the preparation of ZnO NAs.

Recently, with the continuous development of patterning technology, the precise control of the arrays can be realized gradually. ZnO NAs with controllable diameter and period, uniform distribution, and high orientation have been widely used in various energy devices. In this review, we focus on the fabrication techniques of patterned ZnO NAs and their applications in the field of energy conversion.

SYNTHETIC METHODOLOGIES AND PROPERTIES FOR PATTERNED ZnO NAs

Several strategies have been proposed to fabricate highly ordered ZnO NAs, such as nanosphere lithography (NSL) [64–68], electron beam lithography (EBL) [69–72], optical lithography (OL), and laser interference lithography (LIL) techniques [73–80]. Among these, self-assembled NSL is a simple and economical technique, which employs two-dimensional (2D) self-assembled nanometer-sized polystyrene spheres as lithography masks to fabricate patterned arrays [64]. The period and size of the patterned ZnO NAs are dependent on the size of nanospheres [65]. In order to overcome the limitation of period control of this method, heterogeneous NSL was proposed by using two different particles [66]. The conventional NSL required high-temperature post-treatment and had high requirement on the substrate flatness and hydrophobicity. On the other hand, the fabrication of defect-free and period-adjustable ZnO NAs was difficult, owing to the introduction of metal catalyst dots and the inhomogeneous distribution of polystyrene nanospheres [67]. Recently, patterned ZnO NAs were fabricated by an NSL technique that patterns a thickness variation on a polymethyl methacrylate layer [68]. The size of the ZnO NAs was successfully controlled by tuning the etching time under oxygen plasma. The morphology and orientation of ZnO NAs can be effectively controlled by tailoring the thickness of the seed layer and solution concentration. EBL is a high-resolution maskless lithography technique, in which a focused electron beam is used to record predetermined shapes on photoresist (PR) materials [70]. Through this method, highly oriented ZnO NAs with controllable diameter and tunable pattern density were obtained. However, the EBL method was too costly and the processing speed was slow, which was not suitable for large-area periodic ZnO NAs fabrication [72]. Compared with the above methods, OL and LIL techniques are precision processing methods, which combine chemical and physical etching techniques to form the patterned geometry. The OL method uses UV light to transfer a geometric pattern from the photomask to the

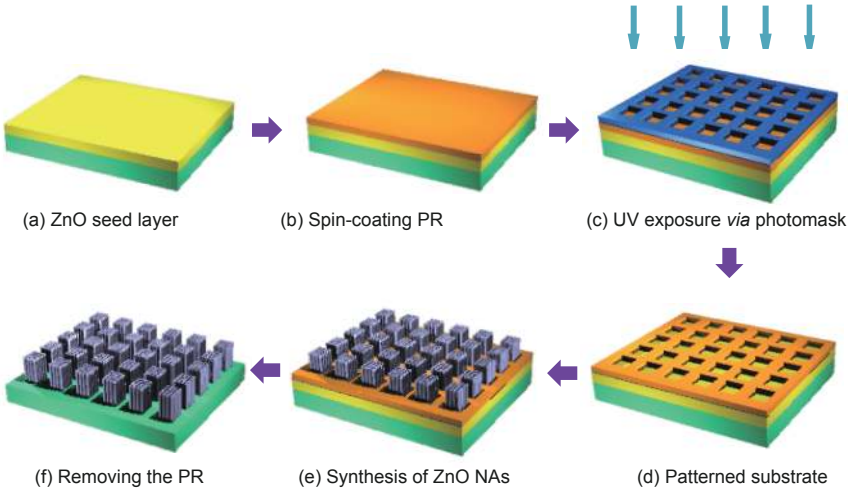

Figure 1 Schematic fabrication process of patterned ZnO NAs by OL method.

PR material. By the OL technique, patterns of various size and shapes on different substrates have been obtained. However, owing to the diffraction effect, the ZnO NAs are usually distributed in clusters instead of individual nanorods, and the nanorod diameter is limited by the incident wavelength [73]. Compared with OL, the LIL technique is a reliable and fast method, which has been widely utilized to obtain nanoscale-patterned ZnO NAs without using a photomask [78]. Generally, an interference pattern is produced by two or multiple coherent lights under one or more exposures, and the irradiated laser energy is recorded on the PR [79]. Then such a pretreated substrate is used to fabricate patterned NAs with controllable density and diameter. Thus, this method allows not only the precise control of the growth cycles and size of the nanorods, but also the successful fabrication of large-area highly oriented ZnO NAs.

Fabrication of patterned ZnO NAs by OL technique

The OL technique is a microfabrication method used to form geometric patterns on substrates. Generally, geometric patterns on masks are transferred to PR materials by light treatment. Fig. 1 shows the typical fabrication processes. First, the PR materials are spin-coated onto the substrate. Second, intense UV light is irradiated onto the substrate with a mask. The light treatment causes a chemical change in positive PR materials, which allows the exposed regions of PR to be removed by solution. For negative PR materials, the unexposed regions become soluble. Thus, the geometric patterns are recorded on the substrate from the mask. Finally, ZnO NAs with different geometric patterns are fabricated. The PR materials are not essential in the OL technique. The geometric patterns can be observed on a photosensitive surface instead of a PR layer [81]. The UV exposure could result in carboxylic acid groups [82] or sulfate anion groups [83] on polycarbonate (PC) films and polyethylene terephthalate (PET) filaments. The acid groups form an acidic environment, which is not conducive to the nucleation and growth of ZnO NAs. Thus, the polymer successfully records the patterns of the mask and is used to grow patterned ZnO NAs. This method enables the direct growth of well-organized ZnO NAs with different patterns.

The OL technique is a simple and effective method for preparing patterned ZnO NAs with different periodicities. The shape, size, and number of ZnO NAs on the substrate can be controlled by changing the fabrication conditions and the photomask.

Fabrication of patterned ZnO NAs by LIL technique

The LIL technique uses a dual-beam laser to design the template patterns [84]. Two-beam laser interference lithography (2BLIL) is used to obtain line template [77]. To obtain various diffraction patterns, multiple exposure processing is employed, as shown in Fig. 2a. Generally, the PR is spin-coated onto a c-oriented ZnO seed layer. Then, 2BLIL processes with single exposure, double exposure at 0°/90°, and triple exposure at −60°/0°/60° are adopted for line, square, and hexagonal lattice arrays, respectively. In 2013, based on the 2BLIL technique, the large-scale patterned ZnO NAs were fabricated on single-crystalline p-GaN substrates through three-exposure modes [85,86]. Such three-exposure modes resulted in different intensity distributions (Fig. 2b–d) and PR tem-

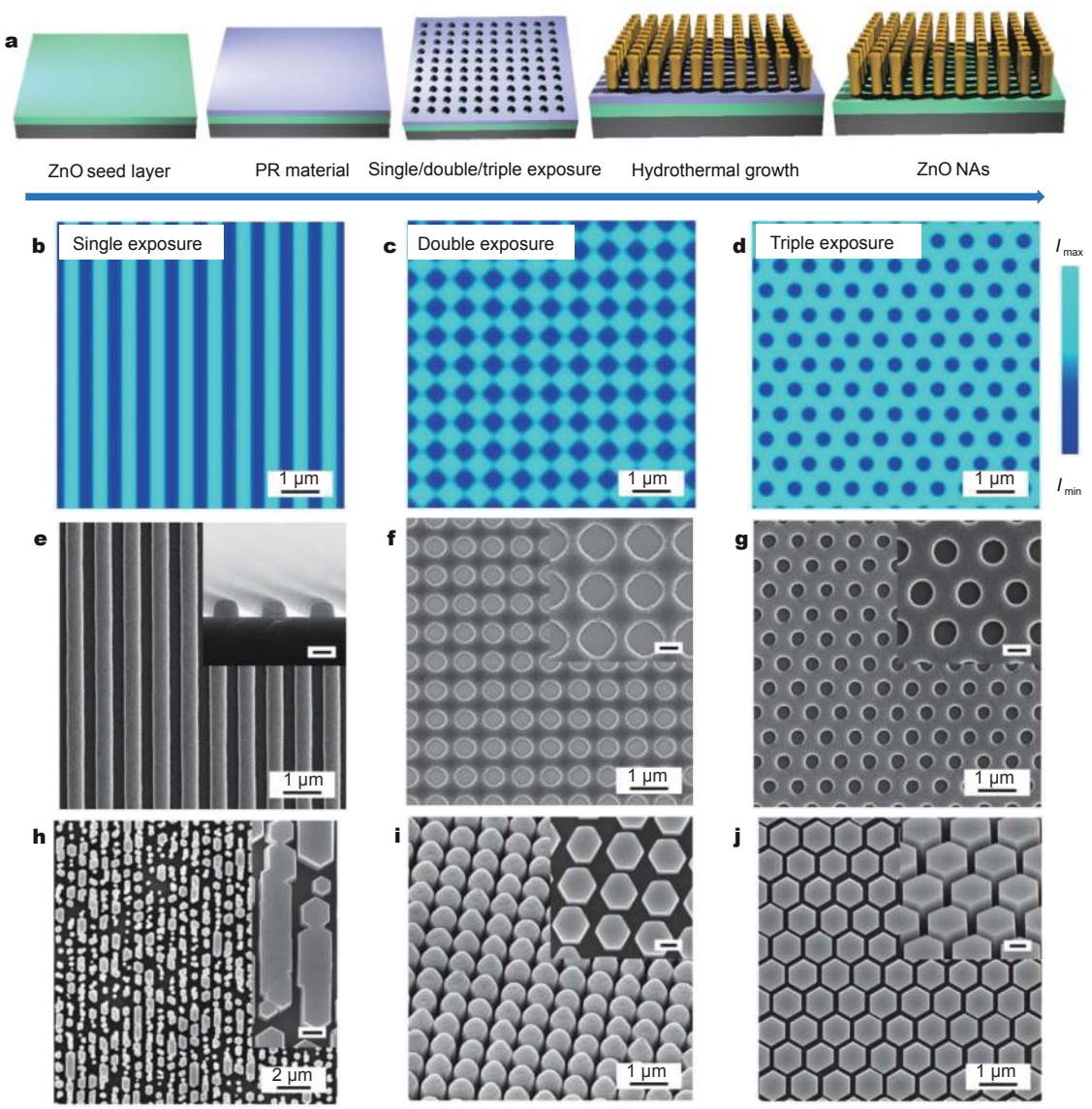

Figure 2 (a) Schematic diagram of patterned ZnO NAs by LIL technique. Simulated exposure intensity distribution of (b) single exposure, (c) double exposure (0° and 90°), and (d) triple exposure (−60°, 0°, and 60°). Such interference patterns can be recorded and the corresponding PR templates are line template (e), hole templates with square symmetry (f), and hexagonal symmetry (g). The corresponding SEM images of patterned ZnO NAs are wall-like ZnO NAs with smooth sidewalls (h), square ZnO NAs with rough-top (i), and hexagonal ZnO NAs with flat-top (j) in a period of 774 nm. All insets show the corresponding magnified SEM images; scale bars are 300 nm. Reprinted with permission from Ref. [85], Copyright 2013, the Royal Society of Chemistry.

plate patterns (Fig. 2e–g). Based on the line templates, the large-scale wall-like patterned ZnO NAs with smooth sidewalls were obtained, as shown in Fig. 2h. The large-scale individual patterned ZnO NAs with square symmetry was also fabricated on a p-GaN substrate by double-exposure processing, as depicted in Fig. 2i. By triple-exposure processing, the ZnO NAs with hexagonal symmetry was prepared on a p-GaN substrate (Fig. 2j). However, the morphology of the patterned ZnO NAs with hexagonal symmetry was influenced by the orientation of the PR template.

In order to fabricate highly ordered ZnO NAs by single-exposure processing, the three-beam laser interference lithography (3BLIL) was proposed [87]. A schematic diagram of the three-beam interferometer system is illustrated in Fig. 3a. The laser beam with a wavelength of 325 nm was first reflected by two dielectric mirrors (M1, M2), and then diverged by a spatial filter. Finally, the

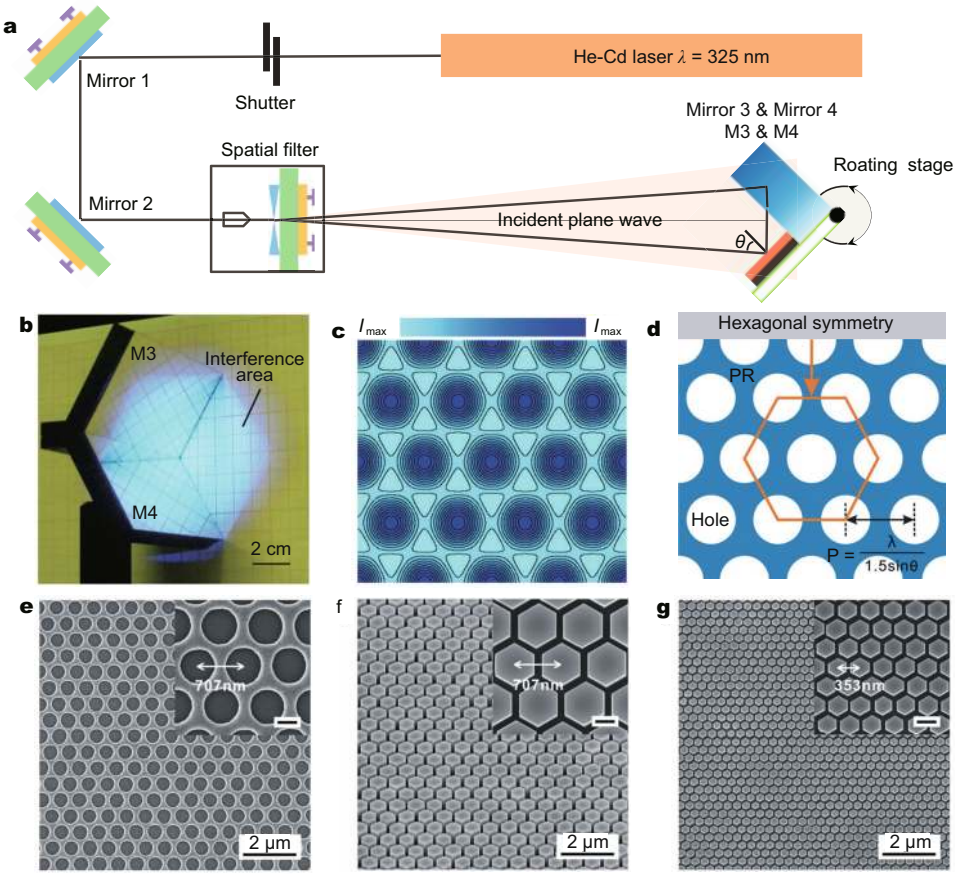

Figure 3 (a) Schematic diagram of the three-beam interferometer system. (b) Optical image of the three-beam Lloyd's mirror interferometer. (c) Simulated intensity distribution of the hexagonal interference pattern. (d) Schematic of the corresponding hexagonal PR hole template by 3BLIL with single exposure. (e) Top-view SEM image of the PR hole template in a period of 707 nm. (f) SEM image of ZnO NAs in the period of 707 nm. (g) Top-view SEM image of the ZnO NAs in a smaller period of 353 nm. Insets show the corresponding magnified SEM images; scale bars are 300 nm. Reprinted with permission from Ref. [87], Copyright 2013, the Royal Society of Chemistry.

incident laser beam was divided into three parts by a three-beam Lloyd's mirror interferometer, which consists of a sample holder, two dielectric mirrors, and a rotating stage, as shown in Fig. 3b. These three laser beams formed a large diamond-shaped exposure area of approximately 22 cm^2, and the irradiated energy was recorded on the PR (Fig. 3d). The corresponding intensity distribution of the hexagonal interference pattern by 3BLIL is illustrated in Fig. 3c. 3BLIL simply fabricated the hole template and the period of ZnO NAs can be continuously controlled. Fig. 3e–g show patterned PR templates and highly ordered ZnO NAs with the different periods. The 3BLIL technique has two advantages compared with the 2BLIL technique. First, 3BLIL is a simple approach to fabricating PR hole templates with hexagonal symmetry through a single exposure without any sample rotation or multiple exposure processes. Second, through 3BLIL, the period of patterned ZnO NAs is successfully decreased from several wavelengths λ to $2\lambda/3$. Periodic regulation can be easily and precisely achieved by rotating the Lloyd's mirror interferometer.

The LIL technique has the advantages of being a maskless and simple process, which is suitable for the fast and large-area fabrication of patterned ZnO NAs. The pattern shape, period, diameter, and distribution can be flexibly controlled by tuning the exposure dosage, beam power, LIL angle, and exposure times. The LIL method is a powerful technique for producing large-area, periodically patterned ZnO NAs and shows great potential for material fabrication.

Optical properties of patterned ZnO NAs

The light absorption properties of ZnO NAs with no pattern, line pattern, and square pattern have been investigated [68,88]. Owing to the light scattering effect, the patterned ZnO NAs show wide absorbance bands com-

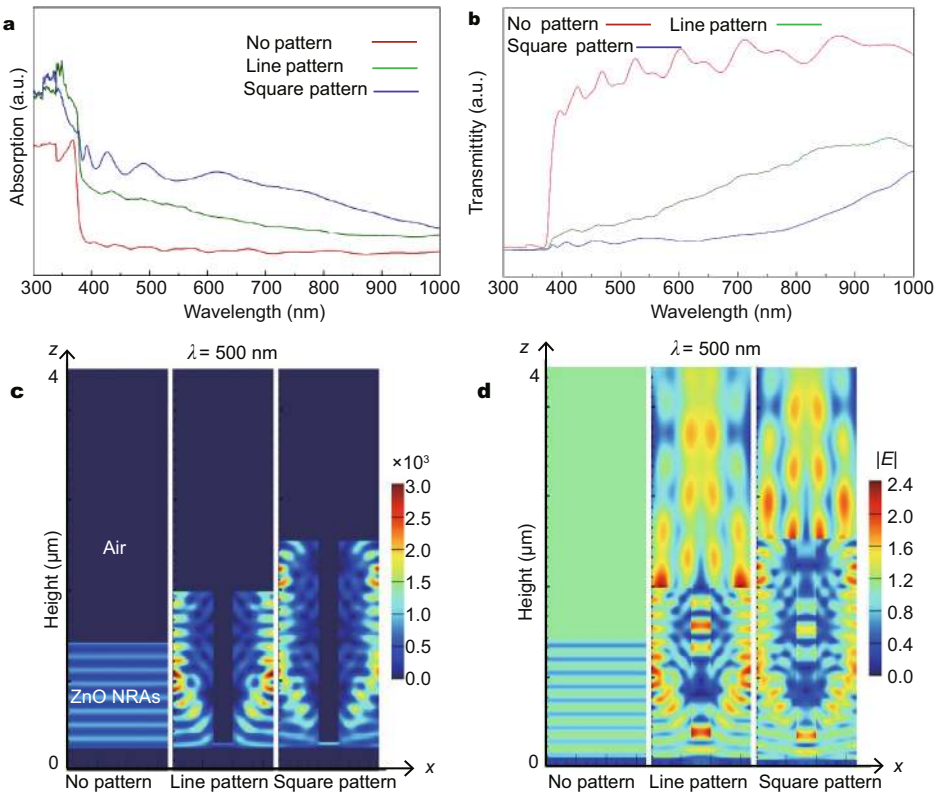

Figure 4 (a) UV-vis-NIR absorption spectra, (b) UV-vis-NIR transmission spectra, (c) simulated cross-sectional optical absorption profiles, and (d) simulated cross-sectional electric-field intensity |E| distributions of the ZnO NAs with no pattern, line pattern, and square pattern, respectively. Simulated profiles used a 500-nm wavelength planar light from the bottom up. Reprinted with permission from Ref. [89], Copyright 2013, American Chemical Society.

pared with the no-pattern samples. The square-patterned ZnO NAs demonstrate the highest absorption among the three samples, as illustrated in Fig. 4a. This result is in good agreement with the transmission spectra in Fig. 4b. The square-patterned ZnO NAs have the maximum absorption and the minimum transmission, indicating an increased optical path length. Two-dimensional finite difference time domain (FDTD) simulations were also performed to understand the light absorption properties. The FDTD simulations allow solving Maxwell's time-dependent equations on a discrete spatial grid. This can be used to analyze the interaction of electromagnetic waves with complex structures in the UV, visible, infrared, terahertz, and microwave frequencies. Three simulation models with different length (1, 1.5, 2 μm) and space (0, 200, 200 nm) were established. The simulation regions were 1 μm × 4 μm in size. The boundary conditions were set as periodic boundary conditions and perfectly matched layer boundary conditions in the *x*-axis and *y*-axis, respectively. A plane-wave light source irradiated the device from the substrate side [89]. As can be seen from Fig. 4c, the light absorption in the patterned ZnO NAs has been enhanced. This is consistent with the observation from the simulated electric-field intensity |*E*| distributions in Fig. 4d. It revealed that the propagation nature of the plane light in the patterned ZnO NAs was enhanced, because of the light reflection and interference in the periodic ZnO NAs. Additionally, the high-frequency structural simulator was used to obtain the optical properties by solving Maxwell's equations [90].

As mentioned above, patterned ZnO NAs with different sizes and periods have different optical properties. The highly controllable and uniform growth of ZnO NAs demonstrates a high application potential for energy devices.

APPLICATIONS OF PATTERNED ZnO NAs IN ENERGY CONVERSION DEVICES

The fabrication of ZnO nanostructures with high light-harvesting capability and large charge-transfer efficiency

is important for highly efficient energy devices [91–96]. Patterned ZnO NAs with adjustable height and controllable period effectively promote light scattering and provide charge transport channels, which have broad application prospects in the field of energy devices [97]. In this review, we summarize the application of patterned ZnO *via* OL and LIL techniques for solar energy, water splitting, light emission devices, and nanogenerators.

Photovoltaic devices

In order to address the global energy crisis, it is vital to exploit abundant, clean, and renewable energy to replace fossil fuels [98–100]. Photovoltaic (PV) technology is able to convert sun's energy to electricity through solar cells [101]. The device performance is closely related to the generation and separation of photogenerated charges [102–105]. To improve the performance of PV solar cells, it is important to fabricate photoanodes with high light-harvesting ability, direct electron transport channel, and efficient carrier collection [106–108].

For dye-sensitized solar cells (DSSCs), the large-scale patterned ZnO–ZnS core–shell NAs were fabricated by using 2BLIL, hydrothermal synthesis, and chemical conversion synthesis methods for the first time [109]. First, a negative PR was spin-coated onto a substrate and the substrate was then annealed for 2 min. Second, the above substrates with top anti-reflective coating were exposed by 2BLIL with different patterns. Third, the patterned ZnO NAs were synthesized in mixed solution of zinc nitrate and hexamethylenetetramine. Finally, the ZnO NAs were immersed in thiacetamide solution to form the ZnS. Four exposure modes were used to obtain the PR template with line, long hexagonal, hexagonal, and square patterns. Compared with other patterned NAs, it is clear that the patterned ZnO–ZnS core–shell NAs with hexagonal symmetry have a large unit density and increased surface area. The UV-vis absorption spectra show that the NAs with hexagonal symmetry have the highest absorption. The enhanced light absorption ability is ascribed to the light scattering effect and increased amount of dye because of the enlarged surface area. The power conversion efficiency (PCE) of the DSSCs was enhanced from 1.11% to 2.09%. The NAs with hexagonal symmetry resulted in the highest PCE and circuit current density with approximately 88% and 60% enhancement. Thus, patterned NAs with tunable arrangement and density are beneficial for efficient DSSCs.

Patterned ZnO NAs were also applied in the ZnO/Cu_2O heterojunction solar cells [89]. Generally, the contact area between ZnO and Cu_2O and the carrier recombination in the materials greatly limited the current density, which further reduced the performance of the solar cells [110–112]. The vertically aligned highly ordered ZnO NAs not only enhanced the light harvesting owing to the light scattering effect, but also increased the carrier collection efficiency owing to the increased heterojunction area [113]. Fig. 5a–c show the top-view and cross-section scanning electron microscopy (SEM) images of three kinds of ZnO NAs. The density clearly varies with the patterns of the NAs. The density of ZnO NAs without pattern has the maximum density of approximately 3.8×10^9 rod cm^{-2}. The density of the ZnO NAs with line and hole patterns are reduced to approximately 2.7×10^9 and 1.2×10^9 rod cm^{-2}, respectively. The corresponding ZnO/Cu_2O heterojunctions are shown in Fig. 5d–f. The Cu_2O films based on the no pattern, line-patterned, and square-patterned ZnO NAs have different grain size, thickness, and heterojunction area. The ordered space of the patterned ZnO NAs was completely filled by Cu_2O, which promotes the generation and separation of carriers in the cells [89]. The light absorption ability has been effectively enhanced owing to the strong light scattering effect. The light-harvesting capability will be further enhanced by increasing the ZnO periods. As illustrated in Fig. 5g, the external quantum efficiency of ZnO/CuO_2 heterojunction cells based on patterned ZnO NAs was significantly increased at 380 nm and reached its peak value at 490 nm. It is clear that the heterojunction based on the square pattern has the highest light absorption. The PV characteristics of the ZnO/CuO_2 solar cells are shown in Fig. 5h. The PCE of the ZnO/Cu_2O heterojunction solar cell based on the square pattern was 2.3 times higher than the reference cells. In particular, the current density increased from 3.29 to 9.89 mA cm^{-2}, which was attributed to the enhanced light harvesting and the efficient carrier collection. Obviously, the period-adjustable ZnO NAs can simultaneously enhance the light absorption and photocarrier collection capability, which is beneficial for efficient solar cells.

Photoelectrochemical devices

The photoelectrochemical (PEC) cell is one of the most promising devices for hydrogen generation, owing to the high theoretical PCE, low cost, and nonpolluting operation [114–119]. PEC cells have two key processes: light trapping and the separation and transport of photogenerated carriers [120,121]. In order to improve the light-harvesting capability, highly ordered square-patterned ZnO NAs were used as the PEC photoanode [122–124]. For no-patterned ZnO NAs, the substrate was di-

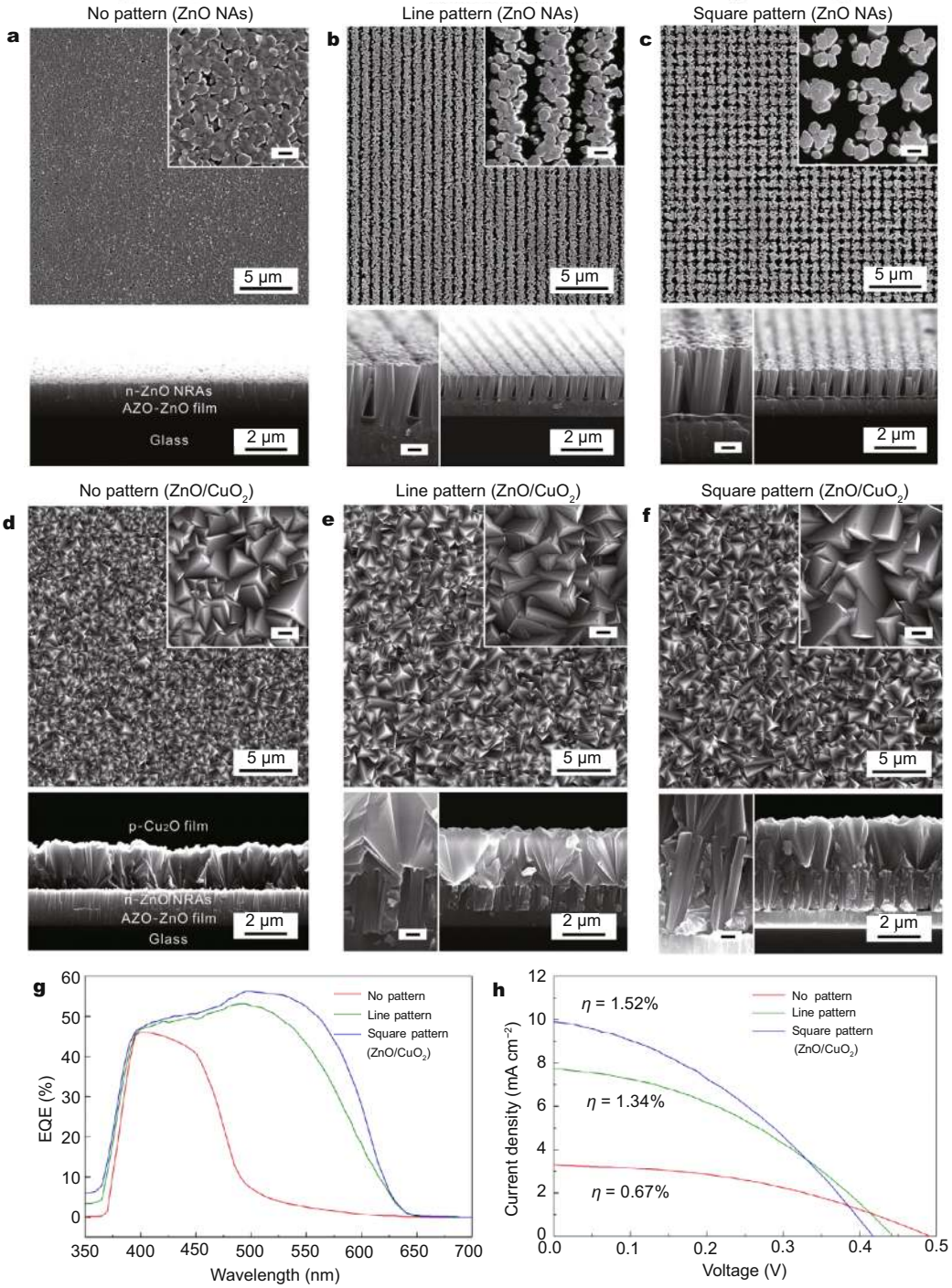

Figure 5 Top and cross-sectional SEM images of the ZnO NAs with no pattern (a), line pattern (b), and square pattern (c). Top and cross-sectional SEM of the ZnO/Cu_2O heterojunctions based on the ZnO NAs with no pattern (d), line pattern (e), and square pattern (f). Insets are the corresponding magnified SEM images with scale bars of 300 nm. External quantum efficiency spectra (g) and current density curves (h) of ZnO/CuO_2 heterojunction cells based on ZnO NAs with different patterns. Reprinted with permission from Ref. [89], Copyright 2013, American Chemical Society.

rectly immersed in the solution with 2.5 mmol zinc nitrate, 2.5 mmol hexamethylenetetramine, and 100 mL deionized water at 95°C for 3 h. For the synthesis of square-patterned ZnO NAs, the PR hole template was first fabricated on the seed layer by the 2BLIL technique. The patterned ZnO NAs were then synthesized by the mentioned hydrothermal method. The patterned ZnO NAs exhibited light scattering properties and induced a large surface area, which simultaneously improved the light-trapping ability and the carrier transport efficiency. The solar to hydrogen conversion efficiency was increased to 0.18%, representing an improvement of 135% [125].

A tree-like three-dimensional (3D) nanowire structure based on patterned ZnO NAs was used as the photoanode, which lengthened the optical paths for light absorption and increased the surface areas for electrochemical reactions [126–129]. The fabrication process of 3D ZnO NAs-CdS is illustrated in Fig. 6a. A patterned PR template fabricated by the LIL technique was used to grow the ZnO NAs. The 3D ZnO NAs were then synthesized by secondary hydrothermal growth. CdS nanoparticles were deposited on the 3D ZnO NAs *via* the ionic layer adsorption reaction (ILAR) method. At last, a thin TiO_2 layer was coated on the above structure by atomic layer deposition (ALD). The CdS nanoparticles and thin TiO_2 layer were deposited onto the 3D structure to increase the light absorption and enhance the photocorrosion resistance. Fig. 6b shows a cross-section SEM image of the patterned ZnO NAs with square symmetry. After the secondary synthesis, the branched ZnO nanowires grew on such patterned ZnO NAs, which contributed to the 3D ZnO nanostructure, as shown in Fig. 6c. Then, the CdS nanoparticles were deposited on the 3D structure. A top-view SEM image of the complex 3D ZnO NAs-CdS is shown in Fig. 6d. This structure has an enlarged roughness factor and improves the light-trapping capacity, which in turn enhances the device performance. Fig. 6e shows that the current density of the 3D ZnO NAs is approximately twice that of the ZnO NAs, owing to the enlarged surface area of the 3D structure. With the CdS layer, the photocurrent density exhibits a significant increase, because of the enhanced visible light absorption. The PCE of the 3D ZnO NAs-CdS devices varied with the deposition thickness of the CdS nanoparticles and achieved a maximum photon-to-hydrogen efficiency of 3.1% [130]. As shown in Fig. 6f, the introduction of the CdS nanoparticles boosts the conversion efficiency, and the highest efficiency is obtained with fifty deposition cycles. The loaded CdS effectively increased the light absorption in visible region. With the CdS nanoparticles, type-II band alignment effectively promoted the carrier separation at the interface [130]. The patterned 3D ZnO NAs offer a large surface area, which is beneficial for loading other materials. Additionally, the tree-like structure provides direct electron transport channels for rapid photogenerated carrier separation and charge transport. Thus, the PEC efficiency was dramatically improved. With respect to device stability, the coated TiO_2 layer protected the photoanode from corrosion [131,132]. As shown in Fig. 6g, the current density of the photoanode with TiO_2 was maintained over 80% of the initial level. Using such 3D structures based on patterned ZnO NAs is considered as a promising protocol to design high-performance PEC devices.

Light emission devices

Light emitting diodes (LEDs) are one of the most promising lighting technologies, and have attracted great attention owing to the demand for displays and illumination [133–135]. ZnO-based solid-state LEDs have been considered as a promising candidate for the next generation of high-efficiency light emitters [136–138]. However, the light extraction efficiency is low [139,140]. Many geometric structures have been used to enhance the light extraction. Periodically aligned ZnO NAs show a periodic modulation of dielectric constant, which could regulate the luminescence property [141]. In 2014, a LIL-patterned PR was used to grow flower-like ZnO NAs by two-phase hydrothermal growth [142]. The patterned ZnO hemisphere array was synthesized by two-step hydrothermal growth. First, a UV-O_3 treatment was performed on the LED substrates with the PR holes, which were then immersed in a mixture of zinc sulfate heptahydrate and ammonium chloride for 15 min to fabricate the flower-like ZnO NAs. Second, the structure was immersed in a solution of zinc sulfate heptahydrate, ammonium chloride and cadmium sulfate hydrate for a second growth. The two-step growth effectively enhanced the lateral directional growth of the ZnO NAs. Compared to a reference LED, the light output of the LED based on the patterned structure was enhanced by 20% at 20 mA. This elevated light extraction efficiency was attributed to the scattering effect of the patterned ZnO NAs.

Generally, the spatial resolution of LEDs is related to the size of the lithography patterns. The patterned ZnO NAs with a diameter of 100 nm derived a resolution of 1.3 μm. Considering the cost, the pore pattern with a diameter of 5 μm was used in flexible LED devices, which yielded a spatial resolution of 7 μm [143]. As illustrated in Fig. 7a, a flexible indium tin oxide (ITO)/PET substrate

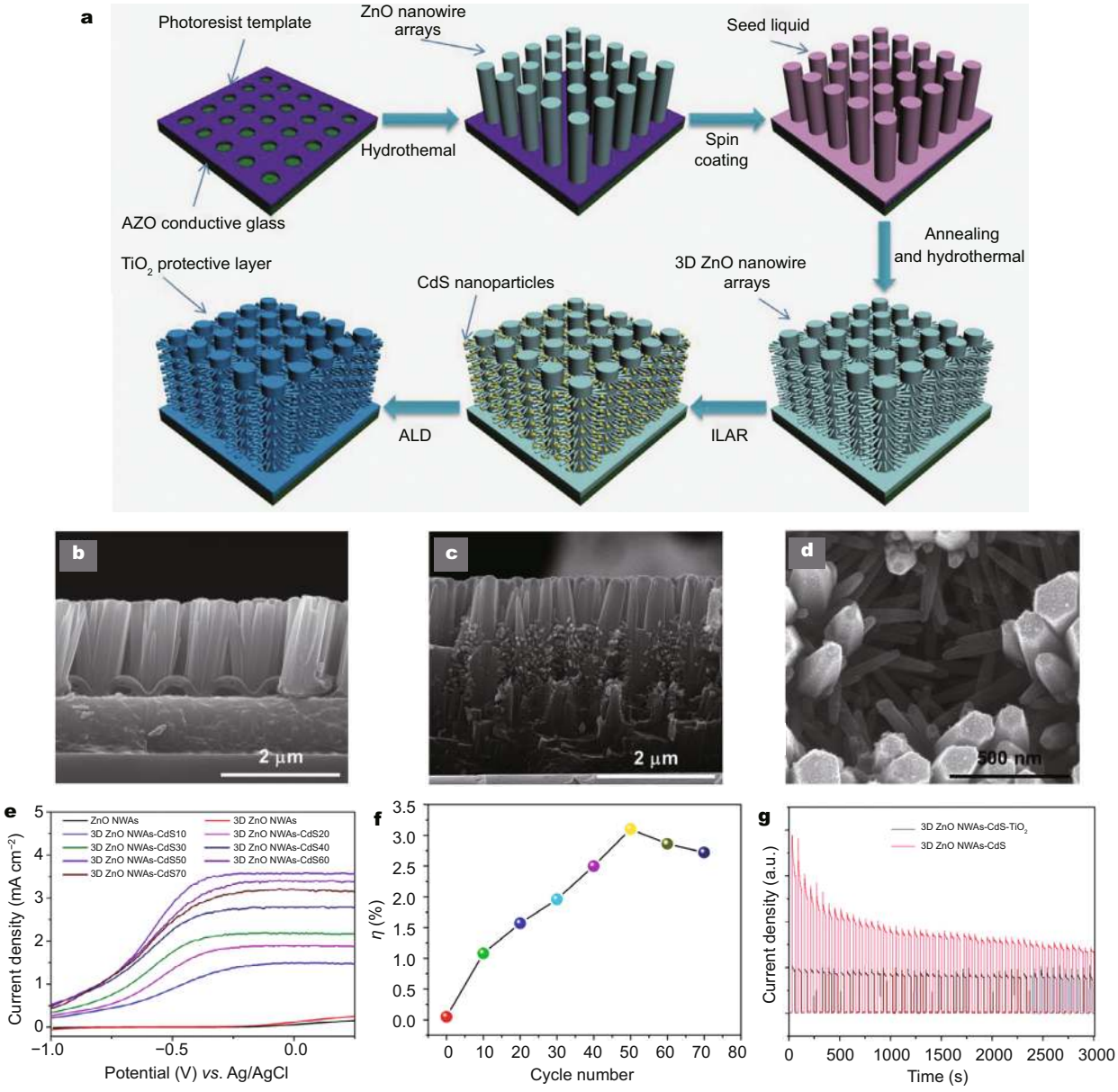

Figure 6 (a) Schematic diagram of the 3D structure fabrication processes. (b) Cross-section SEM image of the patterned ZnO NAs and (c) 3D ZnO NAs. (d) Top-view SEM image of 3D ZnO NAs-CdS. (e) Current density of different ZnO structures with varied CdS deposition cycles. (f) Photon-to-hydrogen efficiency at different CdS deposition cycle numbers. (g) Stability test of the 3D ZnO NAs-CdS and 3D ZnO NAs-CdS-TiO_2 structures. Reprinted with permission from Ref. [130], Copyright 2015, WILEY-VCH Verlag GmbH & Co. KGaA, Weinheim.

with PR was patterned by the OL technique and then the ZnO NAs were fabricated. The space between the ZnO NAs was infiltrated with SU8, but the heads of the ZnO NAs were exposed by oxygen plasma etching. Subsequently, poly(3,4-ethylenedioxythiophene)/polystyrene sulfonate (PEDOT:PSS) was spin-coated onto the ZnO NAs. Finally, an Au film was deposited as a positive electrode of the LED. The OL-patterned ZnO NAs are shown in Fig. 7b–d. The diameter and length of the ZnO nanowires are 300 nm and 4 μm, respectively. Based on such patterned ZnO NAs, a flexible pressure mapping device was fabricated and the corresponding optical images are illustrated in Fig. 7e, f. The electroluminescence performance of the flexible LED based on patterned ZnO NAs is shown in Fig. 7g. The controllable fabrication of patterned ZnO NAs with various periods

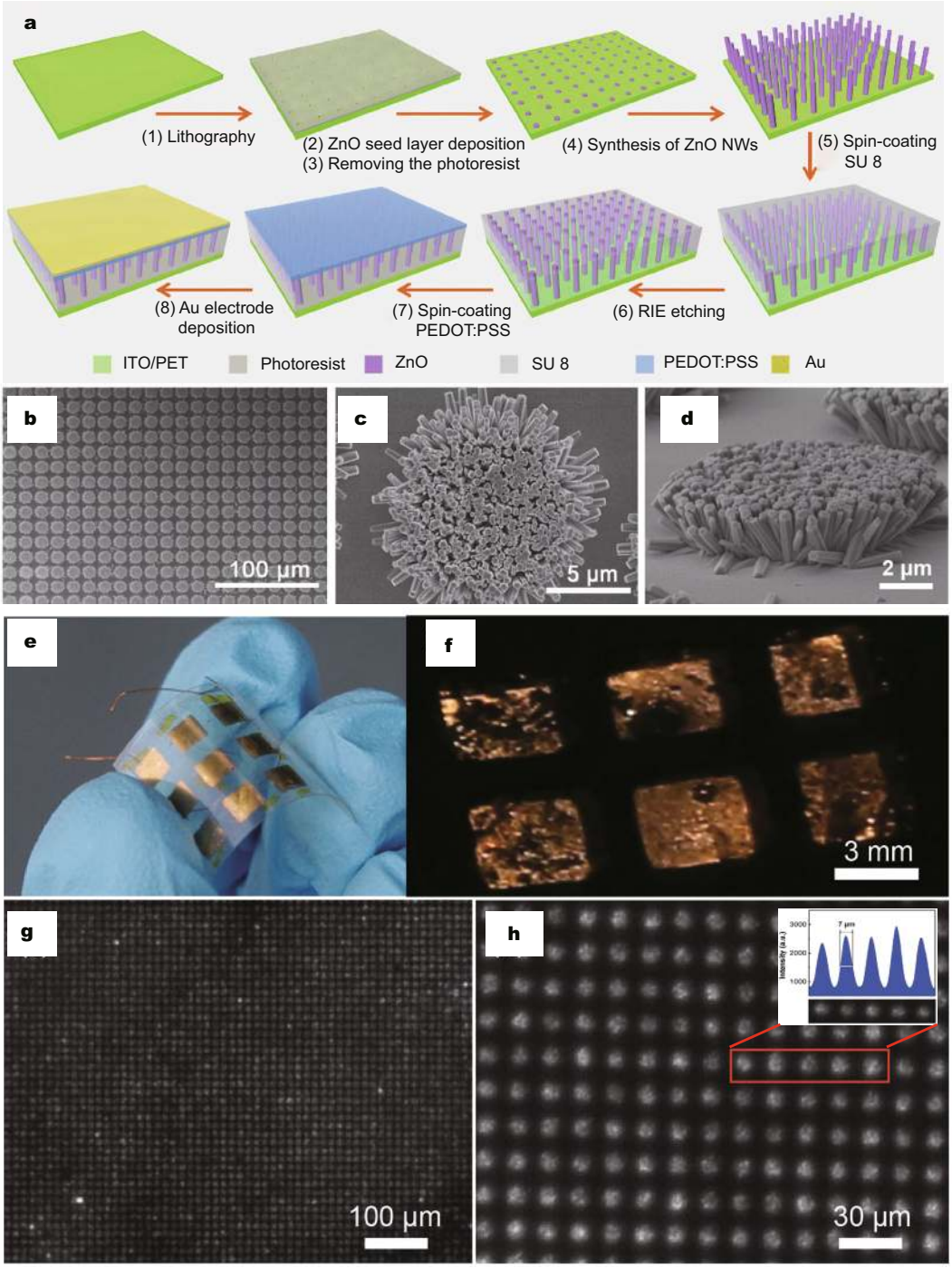

Figure 7 (a) Fabrication process of the patterned ZnO NAs with p-type polymer. (b–d) SEM images of patterned ZnO NAs with different magnification. (e, f) Optical images of the flexible pressure mapping device. (g, h) Optical images of ZnO NAs/p-type polymer LEDs. The inset image shows the five typical LEDs with their emission intensity. Reprinted with permission from Ref. [143], Copyright 2015, WILEY-VCH Verlag GmbH & Co. KGaA, Weinheim.

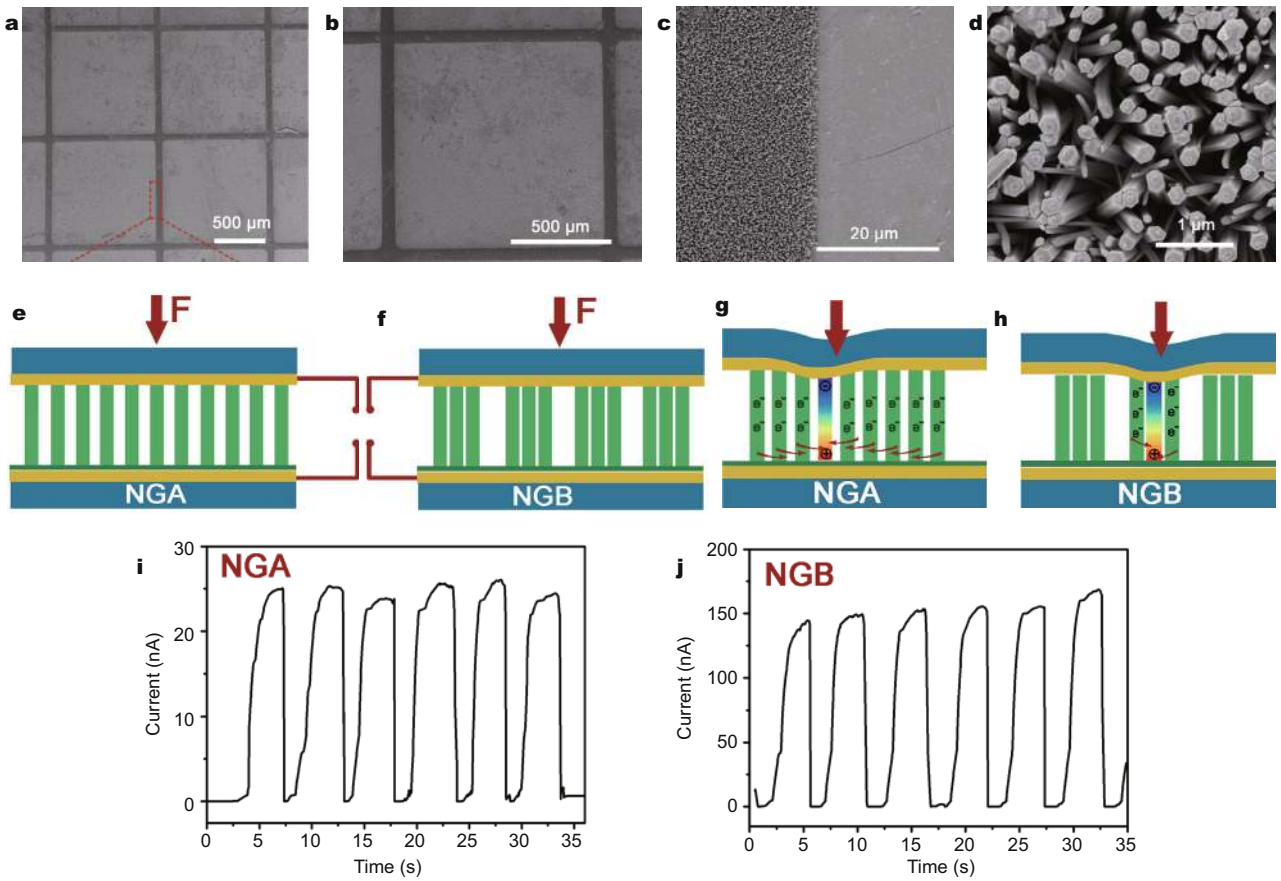

Figure 8 Images showing the surface morphologies of patterned ZnO NAs at low magnification (a, b) and high magnification (c, d). Schematic diagrams of the NGs based on the pristine ZnO NAs (e) and patterned ZnO NAs (f). Working mechanism diagrams (g, h) and current outputs (i, j) of the corresponding NGs. Reprinted with permission from Ref. [158], Copyright 2017, AIP Publishing LLC.

and sizes is beneficial for efficient ZnO-based LED devices. Therefore, the rational design of the pattern structure is essential to improve the efficiency of light extraction [144].

Nanogenerator devices

Nanogenerators (NG) are among the most common devices used to convert mechanical energy produced by mechanical vibration, body movement, airflow, and hydraulic energy into electrical energy at the nanometer scale [145–148]. Vertically aligned ZnO NAs have been widely used in NG devices, by virtue of the piezoelectric effect [149–151]. However, the screening effect on the piezoelectric field induced by the free carriers in ZnO seriously inhibited the output performance of ZnO NAs-based NGs [152–155]. Several strategies have been proposed to reduce the surface free-charges on ZnO NAs, such as the introduction of ZnO p-n homojunctions [156] and doping with lithium [157]. Although the potential screening effect was reduced, the free charges in the unstrained ZnO NAs drifted to neutralize the piezoelectric charges in the strained ZnO NAs, which seriously reduced the device performance. Patterned ZnO NAs provide independent working areas, which effectively inhibit the charge neutralization [158].

Patterned ZnO NAs were fabricated by the OL technique. The surface morphologies of the patterned ZnO NAs are illustrated in Fig. 8a–d. It is clearly evident that the ZnO NAs with a diameter of 50–100 nm were divided to squares with an interval of 20 μm. These patterned ZnO NAs were used to fabricate the NG, which showed a higher output current of 150 nA compared with the pristine ZnO NAs-based NG. Fig. 8e, f show that the space of the patterned ZnO NAs is larger than that of the pristine ZnO NAs. When a compressive strain is applied on the ZnO NAs, positive and negative potentials are produced at the stretched and compressed sides, respectively [159]. The electrons then flow from the ZnO NAs to

the electrode. However, the free charges within the unstrained ZnO NAs will neutralize the piezoelectric charges, as shown in Fig. 8g. The patterned ZnO NAs with independent working areas effectively reduced the screening effect and in turn optimized the output performance with an improvement of six times, as shown in Fig. 8h, j. Therefore, the patterned ZnO NAs with independent working areas provide an effective protocol to enhance the performance of NGs.

CONCLUSIONS AND OUTLOOKS

ZnO has received increasing attention over the past few years because of its excellent properties. Various ZnO nanostructures have been widely used in nanoscale devices. For the improvement of device performances, the accurate control of ZnO structure is particularly important. Several synthetic strategies have been exploited to obtain highly ordered ZnO NAs. The detailed fabrication processes and the advantages of the OL and LIL techniques could offer platforms for the precise control of nanostructure fabrication. Furthermore, we highlight a range of excellent properties associated with different sizes and periods. The relationship between the patterned ZnO NAs and the material properties provides a guide for the selection of nanostructures. In terms of energy conversion applications, the successful integration of patterned ZnO NAs into solar energy, water splitting, light emission devices, and nanogenerators opens a new route to improve the device performances. It is of universal significance for further devotion in the energy conversion device evolution.

Overall, a comprehensive review of the controllable fabrication and functional applications of ZnO NAs by OL and LIL technologies is given. The use of patterning technology is an effective approach for fabricating large-scale highly ordered ZnO NAs with controllable period and diameter, and uniform distribution. Patterned ZnO NAs have direct electron pathways, excellent light-scattering, and enlarged surface area, which are conducive to enhanced light-harvesting ability and accelerated charge transfer in energy devices. Additionally, the segmentation of the patterned ZnO NAs significantly reduced the screening effect in ZnO-based NGs. The applications of the patterned ZnO NAs in energy devices such as solar energy, water splitting, LEDs, and NGs have been summarized. All of the advantages contribute to the enhanced performance of these energy devices. Therefore, the preparation of large-area, low-cost, and high-precision ZnO NAs based on OL and LIL technologies has laid a solid foundation for the development of efficient functional nanodevices. Patterning technology provides an effective approach to fabricating highly efficient devices, which has huge market value and research significance.

Received 2 July 2017; accepted 25 August 2017; published online 5 September 2017

1 Tisdale WA, Williams KJ, Timp BA, *et al.* Hot-electron transfer from semiconductor nanocrystals. Science, 2010, 328: 1543–1547
2 del Alamo JA. Nanometre-scale electronics with III–V compound semiconductors. Nature, 2011, 479: 317–323
3 Zhang Y, Yang Y, Gu Y, *et al.* Performance and service behavior in 1-D nanostructured energy conversion devices. Nano Energ, 2015, 14: 30–48
4 Fortunato E, Barquinha P, Martins R. Oxide semiconductor thin-film transistors: a review of recent advances. Adv Mater, 2012, 24: 2945–2986
5 Banan Sadeghian R, Islam MS, Saif Islam M. Ultralow-voltage field-ionization discharge on whiskered silicon nanowires for gas-sensing applications. Nat Mater, 2011, 10: 135–140
6 Battaglia C, Cuevas A, De Wolf S. High-efficiency crystalline silicon solar cells: status and perspectives. Energ Environ Sci, 2016, 9: 1552–1576
7 Nagarajan L, De Souza RA, Samuelis D, *et al.* A chemically driven insulator–metal transition in non-stoichiometric and amorphous gallium oxide. Nat Mater, 2008, 7: 391–398
8 Yamaguchi S. Main group oxides: making the transition. Nat Mater, 2008, 7: 353–354
9 Kuykendall TR, Schwartzberg AM, Aloni S. Gallium nitride nanowires and heterostructures: toward color-tunable and white-light sources. Adv Mater, 2015, 27: 5805–5812
10 Li A, Zou J, Han X. Growth of III-V semiconductor nanowires and their heterostructures. Sci China Mater, 2016, 59: 51–91
11 Wang ZL. Piezopotential gated nanowire devices: piezotronics and piezo-phototronics. Nano Today, 2010, 5: 540–552
12 Li H, Huang Y, Sun G, *et al.* Directed growth and microwave absorption property of crossed ZnO netlike micro-/nanostructures. J Phys Chem C, 2010, 114: 10088–10091
13 Yang Y, Guo W, Wang X, *et al.* Size dependence of dielectric constant in a single pencil-like ZnO nanowire. Nano Lett, 2012, 12: 1919–1922
14 Zhang Y, Yan X, Yang Y, *et al.* Scanning probe study on the piezotronic effect in ZnO nanomaterials and nanodevices. Adv Mater, 2012, 24: 4647–4655
15 Xu S, Qin Y, Xu C, *et al.* Self-powered nanowire devices. Nat Nanotech, 2010, 5: 366–373
16 Qin Y, Wang X, Wang ZL. Microfibre–nanowire hybrid structure for energy scavenging. Nature, 2008, 451: 809–813
17 Sun X, Gu Y, Wang X, *et al.* Defects energetics and electronic properties of Li doped ZnO: a hybrid hartree-fock and density functional study. Chin J Chem Phys, 2012, 25: 261–268
18 Qi J, Zhang Y, Huang Y, *et al.* Doping and defects in the formation of single-crystal ZnO nanodisks. Appl Phys Lett, 2006, 89: 252115
19 Ma S, Zhang X, Liao Q, *et al.* Enzymatic lactic acid sensing by In-doped ZnO nanowires functionalized AlGaAs/GaAs high electron mobility transistor. Sensors Actuators B-Chem, 2015, 212: 41–46
20 Liu J, Zhang Y, Qi J, *et al.* In-doped zinc oxide dodecagonal

nanometer thick disks. Mater Lett, 2006, 60: 2623–2626
21 Qi J, Zhang H, Lu S, *et al.* High performance indium-doped ZnO gas sensor. J Nanomater, 2015, 2015: 1–6
22 Zhao J, Wang L, Yan X, *et al.* Structure and photocatalytic activity of Ni-doped ZnO nanorods. Mater Res Bull, 2011, 46: 1207–1210
23 Gu Y, Zhang X, Wang X, *et al.* A quantum explanation of the abnormal magnetic behaviour in Mn-doped ZnO nanowires. J Phys-Condens Matter, 2007, 19: 236223
24 Zhang X, Zhang Y, Wang ZL, *et al.* Synthesis and characterization of $Zn_{1-x}Mn_xO$ nanowires. Appl Phys Lett, 2008, 92: 162102
25 Chen H, Qi J, Huang Y, *et al.* Synthesis, structure and properties of Sn-doped ZnO nanobelts. Acta Physico-Chim Sin, 2007, 23: 55–58
26 Tang LD, Zhang Y, Yan XQ, *et al.* Preparation and characteristics of transparent p-type ZnO film by Al and N co-doping method. Appl Surf Sci, 2008, 254: 4508–4511
27 Shen Y, Yan X, Si H, *et al.* Improved photoresponse performance of self-powered ZnO/spiro-MeOTAD heterojunction ultraviolet photodetector by piezo-phototronic effect. ACS Appl Mater Interfaces, 2016, 8: 6137–6143
28 Dai Y, Zhang Y, Li QK, *et al.* Synthesis and optical properties of tetrapod-like zinc oxide nanorods. Chem Phys Lett, 2002, 358: 83–86
29 Leschkies KS, Divakar R, Basu J, *et al.* Photosensitization of ZnO nanowires with CdSe quantum dots for photovoltaic devices. Nano Lett, 2007, 7: 1793–1798
30 Dai Y, Zhang Y, Wang ZL. The octa-twin tetraleg ZnO nanostructures. Solid State Commun, 2003, 126: 629–633
31 Zhang L, Bai S, Su C, *et al.* A high-reliability kevlar fiber-ZnO nanowires hybrid nanogenerator and its application on self-powered UV detection. Adv Funct Mater, 2015, 25: 5794–5798
32 Liao Q, Zhang Z, Zhang X, *et al.* Flexible piezoelectric nanogenerators based on a fiber/ZnO nanowires/paper hybrid structure for energy harvesting. Nano Res, 2014, 7: 917–928
33 Kumar B, Kim SW. Energy harvesting based on semiconducting piezoelectric ZnO nanostructures. Nano Energ, 2012, 1: 342–355
34 Kim D, Lee KY, Gupta MK, *et al.* Self-compensated insulating ZnO-based piezoelectric nanogenerators. Adv Funct Mater, 2014, 24: 6949–6955
35 Liao X, Yan X, Lin P, *et al.* Enhanced performance of ZnO piezotronic pressure sensor through electron-tunneling modulation of MgO nanolayer. ACS Appl Mater Interfaces, 2015, 7: 1602–1607
36 Lin P, Yan X, Zhang Z, *et al.* Self-powered UV photosensor based on PEDOT:PSS/ZnO micro/nanowire with strain-modulated photoresponse. ACS Appl Mater Interfaces, 2013, 5: 3671–3676
37 Wang Z, Qi J, Yan XQ, *et al.* A self-powered strain senor based on a ZnO/PEDOT:PSS hybrid structure. RSC Adv, 2013, 3: 17011–17015
38 Chen S, Lou Z, Chen D, *et al.* Highly flexible strain sensor based on ZnO nanowires and P(VDF-TrFE) fibers for wearable electronic device. Sci China Mater, 2016, 59: 173–181
39 Willander M, Nur O, Zhao QX, *et al.* Zinc oxide nanorod based photonic devices: recent progress in growth, light emitting diodes and lasers. Nanotechnology, 2009, 20: 332001
40 Zhang XM, Lu MY, Zhang Y, *et al.* Fabrication of a high-brightness blue-light-emitting diode using a ZnO-nanowire array grown on p-GaN thin film. Adv Mater, 2009, 21: 2767–2770
41 Liao Q, Liang M, Zhang Z, *et al.* Strain-modulation and service behavior of Au–MgO–ZnO ultraviolet photodetector by piezo-phototronic effect. Nano Res, 2015, 8: 3772–3779
42 Soci C, Zhang A, Xiang B, *et al.* ZnO nanowire UV photodetectors with high internal gain. Nano Lett, 2007, 7: 1003–1009
43 Liao X, Liao Q, Zhang Z, *et al.* A highly stretchable ZnO@fiber-based multifunctional nanosensor for strain/temperature/UV detection. Adv Funct Mater, 2016, 26: 3074–3081
44 Bai S, Wu W, Qin Y, *et al.* High-performance integrated ZnO nanowire UV sensors on rigid and flexible substrates. Adv Funct Mater, 2011, 21: 4464–4469
45 Xue M, Zhou H, Xu Y, *et al.* High-performance ultraviolet-visible tunable perovskite photodetector based on solar cell structure. Sci China Mater, 2017, 60: 407–414
46 Zhang G, Liao Q, Qin Z, *et al.* Fast sensitization process of ZnO-nanorod-array electrodes by electrophoresis for dye-sensitized solar cells. RSC Adv, 2014, 4: 39332–39336
47 Law M, Greene LE, Johnson JC, *et al.* Nanowire dye-sensitized solar cells. Nat Mater, 2005, 4: 455–459
48 Mahmood K, Swain BS, Amassian A. 16.1% Efficient hysteresis-free mesostructured perovskite solar cells based on synergistically improved ZnO nanorod arrays. Adv Energ Mater, 2015, 5: 1500568
49 Zhao H, Wu Q, Hou J, *et al.* Enhanced light harvesting and electron collection in quantum dot sensitized solar cells by TiO_2 passivation on ZnO nanorod arrays. Sci China Mater, 2017, 60: 239–250
50 Young SJ, Liu YH. Field emission properties of Al-doped ZnO nanosheet based on field emitter device with UV exposure. RSC Adv, 2017, 7: 14219–14223
51 Sankaran KJ, Afsal M, Lou SC, *et al.* Electron field emission enhancement of vertically aligned ultrananocrystalline diamond-coated ZnO core-shell heterostructured nanorods. Small, 2014, 10: 179–185
52 Kang Z, Yan X, Wang Y, *et al.* Self-powered photoelectrochemical biosensing platform based on Au NPs@ZnO nanorods array. Nano Res, 2016, 9: 344–352
53 Zhang Y, Kang Z, Yan X, *et al.* ZnO nanostructures in enzyme biosensors. Sci China Mater, 2015, 58: 60–76
54 Kang Z, Gu Y, Yan X, *et al.* Enhanced photoelectrochemical property of ZnO nanorods array synthesized on reduced graphene oxide for self-powered biosensing application. Biosens Bioelectron, 2015, 64: 499–504
55 Kang Z, Yan X, Wang Y, *et al.* Electronic structure engineering of Cu_2O film/ZnO nanorods array all-oxide p-n heterostructure for enhanced photoelectrochemical property and self-powered biosensing application. Sci Rep, 2015, 5: 7882
56 He J, Huang Y, Zhang Y, *et al.* Large-scale synthesis, microstructure and growth mechanism of self-assembled core–shell ZnO/SiO_x nanowires. Mater Lett, 2006, 60: 150–153
57 Yin X, Wang X. Kinetics-driven crystal facets evolution at the tip of nanowires: a new implementation of the Ostwald-Lussac law. Nano Lett, 2016, 16: 7078–7084
58 Li L, Zhai T, Bando Y, *et al.* Recent progress of one-dimensional ZnO nanostructured solar cells. Nano Energ, 2012, 1: 91–106
59 Wu Y, Wang D, Li Y. Understanding of the major reactions in solution synthesis of functional nanomaterials. Sci China Mater, 2016, 59: 938–996
60 Zhang Z, Han X, Zou J. Direct realizing the growth direction of epitaxial nanowires by electron microscopy. Sci China Mater, 2015, 58: 433–440
61 Sun Z, Liao T, Kou L. Strategies for designing metal oxide na-

nostructures. Sci China Mater, 2017, 60: 1–24
62 Nai J, Kang J, Guo L. Tailoring the shape of amorphous nanomaterials: recent developments and applications. Sci China Mater, 2015, 58: 44–59
63 Wang X, Summers CJ, Wang ZL. Large-scale hexagonal-patterned growth of aligned ZnO nanorods for nano-optoelectronics and nanosensor arrays. Nano Lett, 2004, 4: 423–426
64 Li C, Hong G, Wang P, *et al.* Wet chemical approaches to patterned arrays of well-aligned ZnO nanopillars assisted by monolayer colloidal crystals. Chem Mater, 2009, 21: 891–897
65 Ye X, Cai A, Shao J, *et al.* Large area assembly of patterned nanoparticles by a polydimethylsiloxane template. Sci China Mater, 2015, 58: 884–892
66 Seo YH, Kim LH, Kim YB, *et al.* Nanoprobe arrays for multiple single cell insertion using heterogeneous nanosphere lithography (HNSL). Nanoscale, 2013, 5: 7809–7813
67 Zeng H, Xu X, Bando Y, *et al.* Template deformation-tailored ZnO nanorod/nanowire arrays: full growth control and optimization of field-emission. Adv Funct Mater, 2009, 19: 3165–3172
68 Kim SB, Lee WW, Yi J, *et al.* Simple, large-scale patterning of hydrophobic ZnO nanorod arrays. ACS Appl Mater Interfaces, 2012, 4: 3910–3915
69 Lee WW, Kim SB, Yi J, *et al.* Surface polarity-dependent cathodoluminescence in hydrothermally grown ZnO hexagonal rods. J Phys Chem C, 2012, 116: 456–460
70 Zhang D, Wang S, Cheng K, *et al.* Controllable fabrication of patterned ZnO nanorod arrays: investigations into the impacts on their morphology. ACS Appl Mater Interfaces, 2012, 4: 2969–2977
71 Xu S, Wei Y, Kirkham M, *et al.* Patterned growth of vertically aligned ZnO nanowire arrays on inorganic substrates at low temperature without catalyst. J Am Chem Soc, 2008, 130: 14958–14959
72 Kim YJ, Yoo H, Lee CH, *et al.* Position- and morphology-controlled ZnO nanostructures grown on graphene layers. Adv Mater, 2012, 24: 5565–5569
73 Cheng C, Lei M, Feng L, *et al.* High-quality ZnO nanowire arrays directly fabricated from photoresists. ACS Nano, 2009, 3: 53–58
74 Tian Y, Chen H, Zhu X, *et al.* Selective growth and characterization of ZnO nanorods assembled a hexagonal pattern on H_2-decomposed GaN epilayer. Front Optoelectron, 2013, 6: 440–447
75 Lee SH, Parish CM, Xu J. Anisotropic epitaxial ZnO/CdO core/shell heterostructure nanorods. Nanoscale Res Lett, 2012, 7: 626
76 Lin MS, Chen CC, Wang WC, *et al.* Fabrication of the selective-growth ZnO nanorods with a hole-array pattern on a p-type GaN: Mg layer through a chemical bath deposition process. Thin Solid Films, 2010, 518: 7398–7402
77 Kim KS, Jeong H, Jeong MS, *et al.* Polymer-templated hydrothermal growth of vertically aligned single-crystal ZnO nanorods and morphological transformations using structural polarity. Adv Funct Mater, 2010, 20: 3055–3063
78 Miyake M, Chen YC, Braun PV, *et al.* Fabrication of three-dimensional photonic crystals using multibeam interference lithography and electrodeposition. Adv Mater, 2009, 21: 3012–3015
79 Wei Y, Wu W, Guo R, *et al.* Wafer-scale high-throughput ordered growth of vertically aligned ZnO nanowire arrays. Nano Lett, 2010, 10: 3414–3419
80 Yuan D, Guo R, Wei Y, *et al.* Heteroepitaxial patterned growth of vertically aligned and periodically distributed ZnO nanowires on GaN using laser interference ablation. Adv Funct Mater, 2010, 20: 3484–3489
81 Masuda Y, Kinoshita N, Sato F, *et al.* Site-selective deposition and morphology control of UV- and visible-light-emitting ZnO crystals. Cryst Growth Des, 2006, 6: 75–78
82 McCarley RL, Vaidya B, Wei S, *et al.* Resist-free patterning of surface architectures in polymer-based microanalytical devices. J Am Chem Soc, 2005, 127: 842–843
83 Yang P, Zou S, Yang W. Positive and negative ZnO micropatterning on functionalized polymer surfaces. Small, 2008, 4: 1527–1536
84 Morales AM, Lieber CM. A laser ablation method for the synthesis of crystalline semiconductor nanowires. Science, 1998, 279: 208–211
85 Chen X, Yan X, Bai Z, *et al.* Facile fabrication of large-scale patterned ZnO nanorod arrays with tunable arrangement, period and morphology. CrystEngComm, 2013, 15: 8022–8028
86 Morin SA, Amos FF, Jin S. Biomimetic assembly of zinc oxide nanorods onto flexible polymers. J Am Chem Soc, 2007, 129: 13776–13777
87 Chen X, Yan X, Bai Z, *et al.* High-throughput fabrication of large-scale highly ordered ZnO nanorod arrays *via* three-beam interference lithography. CrystEngComm, 2013, 15: 8416–8421
88 Cao F, Tian W, Gu B, *et al.* High-performance UV–vis photodetectors based on electrospun ZnO nanofiber-solution processed perovskite hybrid structures. Nano Res, 2017, 10: 2244–2256
89 Chen X, Lin P, Yan X, *et al.* Three-dimensional ordered ZnO/Cu_2O nanoheterojunctions for efficient metal–oxide solar cells. ACS Appl Mater Interfaces, 2015, 7: 3216–3223
90 Liyanage WPR, Wilson JS, Kinzel EC, *et al.* Fabrication of CdTe nanorod arrays over large area through patterned electrodeposition for efficient solar energy conversion. Sol Energ Mater Sol Cells, 2015, 133: 260–267
91 Li Y, Yan X, Zheng X, *et al.* Fiber-shaped asymmetric supercapacitors with ultrahigh energy density for flexible/wearable energy storage. J Mater Chem A, 2016, 4: 17704–17710
92 Liu S, Liao Q, Lu S, *et al.* Strain modulation in graphene/ZnO nanorod film schottky junction for enhanced photosensing performance. Adv Funct Mater, 2016, 26: 1347–1353
93 Tian W, Zhang C, Zhai T, *et al.* Flexible ultraviolet photodetectors with broad photoresponse based on branched ZnS-ZnO heterostructure nanofilms. Adv Mater, 2014, 26: 3088–3093
94 Sun Y, Yan X, Zheng X, *et al.* Influence of carrier concentration on the resistive switching characteristics of a ZnO-based memristor. Nano Res, 2016, 9: 1116–1124
95 Tian W, Zhai T, Zhang C, *et al.* Low-cost fully transparent ultraviolet photodetectors based on electrospun ZnO-SnO_2 heterojunction nanofibers. Adv Mater, 2013, 25: 4625–4630
96 Sun Y, Yan X, Zheng X, *et al.* High on–off ratio improvement of ZnO-based forming-free memristor by surface hydrogen annealing. ACS Appl Mater Interfaces, 2015, 7: 7382–7388
97 Liu S, Wang L, Feng X, *et al.* Ultrasensitive 2D ZnO piezotronic transistor array for high resolution tactile imaging. Adv Mater, 2017, 29: 1606346
98 Si H, Liao Q, Zhang Z, *et al.* An innovative design of perovskite solar cells with Al_2O_3 inserting at ZnO/perovskite interface for improving the performance and stability. Nano Energ, 2016, 22: 223–231
99 Lewis NS. Research opportunities to advance solar energy utilization. Science, 2016, 351: aad1920–aad1920
100 Si H, Liao Q, Kang Z, *et al.* Deciphering the NH_4PbI_3 intermediate

phase for simultaneous improvement on nucleation and crystal growth of perovskite. Adv Funct Mater, 2017, 499: 1701804
101 Polman A, Knight M, Garnett EC, *et al.* Photovoltaic materials: Present efficiencies and future challenges. Science, 2016, 352: aad4424–aad4424
102 Grätzel M. Dye-sensitized solar cells. J Photochem Photobiol C-Photochem Rev, 2003, 4: 145–153
103 Thavasi V, Renugopalakrishnan V, Jose R, *et al.* Controlled electron injection and transport at materials interfaces in dye sensitized solar cells. Mater Sci Eng-R-Rep, 2009, 63: 81–99
104 Bouclé J, Ackermann J. Solid-state dye-sensitized and bulk heterojunction solar cells using TiO_2 and ZnO nanostructures: recent progress and new concepts at the borderline. Polym Int, 2012, 61: 355–373
105 Li LB, Wu WQ, Rao HS, *et al.* Hierarchical ZnO nanorod-on-nanosheet arrays electrodes for efficient CdSe quantum dot-sensitized solar cells. Sci China Mater, 2016, 59: 807–816
106 Yu M, Long YZ, Sun B, *et al.* Recent advances in solar cells based on one-dimensional nanostructure arrays. Nanoscale, 2012, 4: 2783–2796
107 Chen T, Hu W, Song J, *et al.* Interface functionalization of photoelectrodes with graphene for high performance dye-sensitized solar cells. Adv Funct Mater, 2012, 22: 5245–5250
108 Kim J, Koh JK, Kim B, *et al.* Nanopatterning of mesoporous inorganic oxide films for efficient light harvesting of dye-sensitized solar cells. Angew Chem Int Ed, 2012, 51: 6864–6869
109 Chen X, Bai Z, Yan X, *et al.* Design of efficient dye-sensitized solar cells with patterned ZnO–ZnS core–shell nanowire array photoanodes. Nanoscale, 2014, 6: 4691–4697
110 Zoolfakar AS, Rani RA, Morfa AJ, *et al.* Enhancing the current density of electrodeposited ZnO–Cu_2O solar cells by engineering their heterointerfaces. J Mater Chem, 2012, 22: 21767–21775
111 Marin AT, Muñoz-Rojas D, Iza DC, *et al.* Novel atmospheric growth technique to improve both light absorption and charge collection in ZnO/Cu_2O thin film solar cells. Adv Funct Mater, 2013, 23: 3413–3419
112 Lee YS, Heo J, Siah SC, *et al.* Ultrathin amorphous zinc-tin-oxide buffer layer for enhancing heterojunction interface quality in metal-oxide solar cells. Energ Environ Sci, 2013, 6: 2112–2118
113 Cui J, Gibson UJ. A simple two-step electrodeposition of Cu_2O/ZnO nanopillar solar cells. J Phys Chem C, 2010, 114: 6408–6412
114 Liu J, Liu Y, Liu N, *et al.* Metal-free efficient photocatalyst for stable visible water splitting *via* a two-electron pathway. Science, 2015, 347: 970–974
115 Liu Y, Gu Y, Yan X, *et al.* Design of sandwich-structured ZnO/ZnS/Au photoanode for enhanced efficiency of photoelectrochemical water splitting. Nano Res, 2015, 8: 2891–2900
116 Wang W, Tadé MO, Shao Z. Research progress of perovskite materials in photocatalysis- and photovoltaics-related energy conversion and environmental treatment. Chem Soc Rev, 2015, 44: 5371–5408
117 Liu Y, Kang Z, Si H, *et al.* Cactus-like hierarchical nanorod-nanosheet mixed dimensional photoanode for efficient and stable water splitting. Nano Energ, 2017, 35: 189–198
118 Marschall R. Semiconductor composites: strategies for enhancing charge carrier separation to improve photocatalytic activity. Adv Funct Mater, 2014, 24: 2421–2440
119 Wu F, Cao F, Liu Q, *et al.* Enhancing photoelectrochemical activity with three-dimensional p-CuO/n-ZnO junction photocathodes. Sci China Mater, 2016, 59: 825–832
120 Cao S, Yan X, Kang Z, *et al.* Band alignment engineering for improved performance and stability of $ZnFe_2O_4$ modified CdS/ZnO nanostructured photoanode for PEC water splitting. Nano Energ, 2016, 24: 25–31
121 Yu Y, Zhang Z, Yin X, *et al.* Enhanced photoelectrochemical efficiency and stability using a conformal TiO_2 film on a black silicon photoanode. Nat Energ, 2017, 2: 17045
122 Bai Z, Zhang Y. CdS nanoparticles sensitized large-scale patterned ZnO nanowire arrays for enhanced solar water splitting. J Solid State Electrochem, 2016, 20: 3499–3505
123 Liu Y, Yan X, Kang Z, *et al.* Synergistic effect of surface plasmonic particles and surface passivation layer on ZnO nanorods array for improved photoelectrochemical water splitting. Sci Rep, 2016, 6: 29907
124 Zhao K, Yan X, Gu Y, *et al.* Self-powered photoelectrochemical biosensor based on CdS/RGO/ZnO nanowire array heterostructure. Small, 2016, 12: 245–251
125 Hu Y, Yan X, Gu Y, *et al.* Large-scale patterned ZnO nanorod arrays for efficient photoelectrochemical water splitting. Appl Surf Sci, 2015, 339: 122–127
126 Kargar A, Sun K, Jing Y, *et al.* Tailoring n-ZnO/p-Si branched nanowire heterostructures for selective photoelectrochemical water oxidation or reduction. Nano Lett, 2013, 13: 3017–3022
127 Qiu Y, Yan K, Deng H, *et al.* Secondary branching and nitrogen doping of ZnO nanotetrapods: building a highly active network for photoelectrochemical water splitting. Nano Lett, 2012, 12: 407–413
128 Zhang X, Liu Y, Kang Z. 3D branched ZnO nanowire arrays decorated with plasmonic Au nanoparticles for high-performance photoelectrochemical water splitting. ACS Appl Mater Interfaces, 2014, 6: 4480–4489
129 Yang JS, Wu JJ. Low-potential driven fully-depleted $BiVO_4$/ZnO heterojunction nanodendrite array photoanodes for photoelectrochemical water splitting. Nano Energ, 2017, 32: 232–240
130 Bai Z, Yan X, Li Y, *et al.* 3D-branched ZnO/CdS nanowire arrays for solar water splitting and the service safety research. Adv Energ Mater, 2016, 6: 1501459
131 Chen W, Qiu Y, Yang S. Branched ZnO nanostructures as building blocks of photoelectrodes for efficient solar energy conversion. Phys Chem Chem Phys, 2012, 14: 10872–10881
132 Sun K, Jing Y, Li C, *et al.* 3D branched nanowire heterojunction photoelectrodes for high-efficiency solar water splitting and H_2 generation. Nanoscale, 2012, 4: 1515–1521
133 Wierer JJ, David A, Megens MM. III-nitride photonic-crystal light-emitting diodes with high extraction efficiency. Nat Photon, 2009, 3: 163–169
134 Nadarajah A, Word RC, Meiss J, *et al.* Flexible inorganic nanowire light-emitting diode. Nano Lett, 2008, 8: 534–537
135 Bao R, Wang C, Peng Z, *et al.* Light-emission enhancement in a flexible and size-controllable ZnO nanowire/organic light-emitting diode array by the piezotronic effect. ACS Photonics, 2017, 4: 1344–1349
136 Li X, Liang R, Tao J, *et al.* Flexible light emission diode arrays made of transferred Si microwires-ZnO nanofilm with piezo-phototronic effect enhanced lighting. ACS Nano, 2017, 11: 3883–3889
137 Shi ZF, Sun XG, Wu D, *et al.* High-performance planar green light-emitting diodes based on a PEDOT:PSS/$CH_3NH_3PbBr_3$/ZnO sandwich structure. Nanoscale, 2016, 8: 10035–10042
138 Li X, Qi J, Zhang Q, *et al.* Saturated blue-violet electro-

luminescence from single ZnO micro/nanowire and p-GaN film hybrid light-emitting diodes. Appl Phys Lett, 2013, 102: 221103
139 Yang Q, Liu Y, Pan C, *et al.* Largely enhanced efficiency in ZnO nanowire/p-polymer hybridized inorganic/organic ultraviolet light-emitting diode by piezo-phototronic effect. Nano Lett, 2013, 13: 607–613
140 Shen Y, Chen X, Yan X, *et al.* Low-voltage blue light emission from n-ZnO/p-GaN heterojunction formed by RF magnetron sputtering method. Curr Appl Phys, 2014, 14: 345–348
141 Kee CS, Ko DK, Lee J. Photonic band gaps of two-dimensional ZnO nanorod photonic crystals. J Phys D-Appl Phys, 2005, 38: 3850–3853
142 Lee R, Jeong H, Pak Y, *et al.* Fabrication of zinc oxide hemispheres array and its application into solid state LEDs. Sci Adv Mater, 2014, 6: 2465–2469
143 Bao R, Wang C, Dong L, *et al.* Flexible and controllable piezo-phototronic pressure mapping sensor matrix by ZnO NW/p-polymer LED array. Adv Funct Mater, 2015, 25: 2884–2891
144 Gu W, Song P, Yin L, *et al.* Improved light extraction of GaN-based LED with patterned Ga-doped ZnO transparent conducting layer. Mol Crysts Liquid Crysts, 2016, 626: 231–237
145 Li W, Torres D, Díaz R, *et al.* Nanogenerator-based dual-functional and self-powered thin patch loudspeaker or microphone for flexible electronics. Nat Commun, 2017, 8: 15310
146 Peng W, Wang X, Yu R, *et al.* Enhanced performance of a self-powered organic/inorganic photodetector by pyro-phototronic and piezo-phototronic effects. Adv Mater, 2017, 29: 1606698
147 Yang Y, Pradel KC, Jing Q, *et al.* Thermoelectric nanogenerators based on single Sb-doped ZnO micro/nanobelts. ACS Nano, 2012, 6: 6984–6989
148 Wang X, Song J, Liu J, *et al.* Direct-current nanogenerator driven by ultrasonic waves. Science, 2007, 316: 102–105
149 Zhou J, Fei P, Gu Y, *et al.* Piezoelectric-potential-controlled polarity-reversible Schottky diodes and switches of ZnO wires. Nano Lett, 2008, 8: 3973–3977
150 Wang ZL, Song J. Piezoelectric nanogenerators based on zinc oxide nanowire arrays. Science, 2006, 312: 242–246
151 Wu W, Wang ZL. Piezotronic nanowire-based resistive switches as programmable electromechanical memories. Nano Lett, 2011, 11: 2779–2785
152 Lee KY, Bae J, Kim SM, *et al.* Depletion width engineering *via* surface modification for high performance semiconducting piezoelectric nanogenerators. Nano Energ, 2014, 8: 165–173
153 Liu J, Fei P, Song J, *et al.* Carrier density and Schottky barrier on the performance of DC nanogenerator. Nano Lett, 2008, 8: 328–332
154 Shin DM, Tsege EL, Kang SH, *et al.* Freestanding ZnO nanorod/graphene/ZnO nanorod epitaxial double heterostructure for improved piezoelectric nanogenerators. Nano Energ, 2015, 12: 268–277
155 Sun Y, Yan X, Zheng X, *et al.* Effect of carrier screening on ZnO-based resistive switching memory devices. Nano Res, 2017, 10: 77–86
156 Pradel KC, Wu W, Ding Y, *et al.* Solution-derived ZnO homojunction nanowire films on wearable substrates for energy conversion and self-powered gesture recognition. Nano Lett, 2014, 14: 6897–6905
157 Sohn JI, Cha SN, Song BG, *et al.* Engineering of efficiency limiting free carriers and an interfacial energy barrier for an enhancing piezoelectric generation. Energ Environ Sci, 2013, 6: 97–104
158 Yang D, Qiu Y, Jiang Q, *et al.* Patterned growth of ZnO nanowires on flexible substrates for enhanced performance of flexible piezoelectric nanogenerators. Appl Phys Lett, 2017, 110: 063901
159 Romano G, Mantini G, Di Carlo A, *et al.* Piezoelectric potential in vertically aligned nanowires for high output nanogenerators. Nanotechnology, 2011, 22: 465401

Acknowledgements This work was supported by the National Key Research and Development Program of China (2013CB932602 and 2016YFA0202701), the Program of Introducing Talents of Discipline to Universities (B14003), the National Natural Science Foundation of China (51527802, 51232001, 51372020 and 51602020), Beijing Municipal Science & Technology Commission (Z151100003315021), and China Postdoctoral Science Foundation (2016M600039).

Author contributions Si H and Kang Z contributed equally to this work. Si H and Kang Z wrote the manuscript under the guidance of Zhang Y. Zhang Y, Liao Q and Zhang Z investigated and analyzed the literatures. Wang L and Zhang Y proposed and supervised the review designing, and contributed to the general discussion and article revision. All authors discussed and provided feedback on the manuscripts structure, arguments and conclusions.

Conflict of interest The authors declare that they have no conflict of interest.

Yue Zhang is a professor of material physics at the University of Science and Technology Beijing, China. His research focuses on functional nano-materials and nano-devices, novel energy harvesting devices and sensing devices, as well as nanoscale failure and service behavior. Prof. Yue Zhang has conducted or participated in more than 50 major research projects from the central and local governments of China, and has been awarded the financial support for Outstanding Young Scientist Foundation of China and selected as the chief scientist of Major National Scientific Research Projects. He has published more than 400 papers in peer reviewed scientific journals with more than 7000 citations. He has also published 8 monographs, and applied for over 70 patents with 37 authorizations.

图案化ZnO纳米结构的设计调控及其在能量转换器件中的应用

司浩楠[1†], 康卓[1†], 廖庆亮[1], 张铮[1], 张晓梅[2], 汪莉[3*], 张跃[1,4*]

摘要 ZnO作为典型的直接带隙宽禁带半导体材料具有丰富的形貌结构和独特的物理、化学性能，被广泛应用于能源、信息技术、生物医学等领域. 目前纳米结构的精确设计与可控制备已成为改善ZnO基功能型纳器件性能的重要手段. 本论文介绍了利用图案化技术对ZnO纳米结构进行限域生长的技术手段，重点综述了光刻技术和激光干涉模板法在精细ZnO纳米结构制备方面的研究进展，及其在光伏电池、光电化学电池、发光器件和纳米发电机四种能量转换器件中的应用. 形貌结构可调的ZnO纳米结构具有分立的高精度空间纳米结构、增大的比表面积、提升的光子捕获能力, 在与其他材料复合时利于实现高效的载流子行为调控, 获得了高效的能量转换, 满足了不同功能型纳器件对材料结构的需求. 针对ZnO纳米结构精确设计所发展的一系列图案化技术对其他材料的复杂纳米结构可控制备具有重要的指导意义, 亦为功能型纳器件的进一步发展开辟了一个全新的途径.